

## Effects of surface and physical confinement on the phase transitions of cyclohexane in porous silica

R. Mu and V. M. Malhotra

*Department of Physics and Molecular Science Program, Southern Illinois University at Carbondale, Carbondale, Illinois 62901-4401*

(Received 14 February 1991)

We have measured the specific heat ( $C_p$ ) of cyclohexane at  $120 < T < 300$  K when cyclohexane was physically restricted in porous Spherosil (silica) samples of pore radii 4, 7.5, 15, 30, and 62.5 nm. The behaviors of the monoclinic-to-cubic structural transition and of the melting transition of cyclohexane were determined. As expected, both transition temperatures, i.e., solid-solid and melting, inversely scaled with the pore radius ( $R_p$ ). It is argued that the surface heterogeneity, the presence of hydroxyl groups, and the radius of curvature (especially for smaller pores) induce considerable disorder in the adsorbed layers of cyclohexane, thus, resulting in the nucleation of crystalline grains of various sizes rather than in a single crystalline plug of cyclohexane in the porous silica samples. The distribution of the grain boundaries of crystalline cyclohexane produces a specific-heat peak for the melting transition, which almost resembles the  $\lambda$  shape for  $R_p \leq 30$  nm. Unlike the monoclinic-to-cubic transition, the  $\lambda$  anomaly of the melting transition does not reflect a logarithmic dependence near the transition temperature. It is also argued, from the comparative observed  $C_p$  behavior of the bulk cyclohexane with the physically restricted cyclohexane, that the cyclohexane liquid is more viscous than the bulk when it is confined in pores of 4 and 7.5 nm.

### INTRODUCTION

Thermodynamic and dynamic properties of fluids are considerably altered relative to their bulk state when the fluids are physically confined in ultrasmall pores ( $< 100$  nm).<sup>1-7</sup> Awschalom and his co-workers<sup>1</sup> systematically examined the effects of geometrical confinement on the supercooling of liquid oxygen in porous sol-gel glasses and found the freezing transition temperature ( $T_f$ ) was depressed in comparison to the bulk. Based on the plug model they demonstrated that  $\Delta T_f$  ( $\Delta T_f = T_0 - T_f$ , where  $T_0$  is the bulk freezing temperature of the fluid and  $T_f$  is the freezing temperature of the fluid in the porous sol-gel glass) inversely scales with a single length scale, i.e., the mean pore radius  $R_p$ . The observed undercooling and hysteretic behavior of the freezing of liquid oxygen in porous glass has been associated with freezing nucleation not being initiated at the pore walls. Awschalom and Warnock<sup>1</sup> argued that a similar undercooling effect should also hold for solid-solid transition in ultrasmall pores. Consistent with this argument, Mu and Malhotra,<sup>6</sup> from their transmission infrared measurements at  $100 \text{ K} < T < 300 \text{ K}$  on cyclohexane confined in porous ( $< 40$  nm) KBr cylindrical disk, reported that the melting transition ( $T_m$ ) and the monoclinic-to-cubic structural transition (solid-solid transition,  $T_s$ ) temperatures of cyclohexane were depressed relative to those detected for the bulk. Jackson and McKenna<sup>7</sup> observed, using their differential scanning calorimetry (DSC) results on various nonpolar organic fluids confined in surface-treated porous glass, that not only the  $T_m$  but also even the glass transition ( $T_g$ ) temperature inversely scale with  $R_p$ . Although the aforementioned studies have led to a better understanding of the thermodynamic behavior of fluids in ultrasmall pores, the results and interpretations are still

controversial.<sup>1,3</sup> In addition to the role the finite-size effects<sup>8</sup> play on the thermodynamic and dynamic properties of a confined fluid, the roles of the surface structure of the confining media, of the surface heterogeneity and surface roughness, of the surface-fluid interactions, and of the size and shape are not well understood.

In this paper we report the effects of physical confinement and the surface of the confining media on the melting transition and on the monoclinic-to-cubic transition of cyclohexane when cyclohexane is restricted in porous silica of pore radii 4, 7.5, 15, 30, and 62.5 nm. This was accomplished by measuring the specific heat of cyclohexane at  $120 \text{ K} < T < 300 \text{ K}$  in porous silica with the help of the DSC technique. We chose cyclohexane to comprehend the above-mentioned effects because (i) cyclohexane is a nonpolar molecule which should mitigate strong surface-fluid interactions (ii) cyclohexane has well-defined solid-liquid (280 K) and solid-solid (186 K) phase transitions;<sup>9,10</sup> (iii) cyclohexane's structure and its thermodynamic properties are documented<sup>11-13,10,14</sup> in all three condensed phases, i.e., monoclinic phase ( $T < 186 \text{ K}$ ), cubic phase ( $186 \text{ K} < T < 280 \text{ K}$ ), and liquid phase ( $280 \text{ K} < T < 351 \text{ K}$ ); and (iv) cyclohexane is a typical "globular" organic compound which has considerable molecular rotational and reorientational motion in its cubic solid phase. Also, the monoclinic-to-cubic phase transition is characterized as a rotational order-disorder transition. Therefore, we believe cyclohexane can serve as an excellent probe to gauge physical confinement and surface effects.

### EXPERIMENTAL

In order to evaluate the spatial restriction and interfacial interaction effects on the solid-liquid and solid-solid transitions of cyclohexane, five different pore-sized

Spherosils were commercially obtained from Phase Separations, Inc. (USA). Spherosil samples, composed of pure silica, were in the form of spherical beads of diameters 75–150  $\mu\text{m}$ . Each sample has been characterized<sup>15</sup> for its average pore size and specific surface area. The physical characteristics of the samples have been summarized in Table I.

According to the manufacturer, the silica samples are free of impurities and contamination. However, we adopted the previously reported<sup>2</sup> cleaning procedures to ensure a uniformity of the five different pore-sized Spherosils. The cleaning of the silica beads and the sample preparation procedures utilized are briefly summarized. (a) Each sample was first soaked in  $\text{H}_2\text{O}_2$  solution for 48 h and then extensively rinsed with isopropanol, acetone, and deionized distilled water to eliminate organic impurities. (b) Efforts were made to remove any inorganic contaminants by treating the glass beads with  $\text{HNO}_3$  acid for 48 h. After the acid treatment, the beads were thoroughly washed with deionized distilled water. (c) The wet glass beads were transferred to a vacuum-tight quartz-glass tube assembly mounted in a high temperature furnace. The samples were first dried under vacuum at room temperature and then were stepwise heated to 723 K. The vacuum drying at 723 K was continued for 8 h to desorb water and hydroxyl groups from the silica surface. The samples were cooled to room temperature under vacuum, made vacuum tight by shutting off the stopcock, and then moved to a nitrogen-purged dry box. (d) A known quantity of ultrapure cyclohexane (99.9% purity, obtained from Aldrich) was injected into the sealed sample compartment with the help of a syringe. The cyclohexane was allowed to diffuse into the pores for at least 4 h. (e) Each sample from step (d) was loaded into 10 preweighed Al DSC volatile pans. The sample pans were subjected to various drying times, and only those pans which showed very little excess bulk cyclohexane in the filled pore state were chosen for further specific-heat measurements. The DSC scans were recorded at  $120 \text{ K} < T < 300 \text{ K}$  at which time the transition temperatures and their associated enthalpies were monitored. Consistent with the observation of Torii *et al.*,<sup>2</sup> we found that if the pores are partially filled then the transition temperatures and their enthalpies are more depressed in comparison to the completely filled state.

The specific heat of samples containing cyclohexane was measured at  $120 \text{ K} < T < 300 \text{ K}$  using a well-calibrated<sup>16,17</sup> Perkin Elmer DSC7 system fitted with a low temperature accessory. The data were collected at a

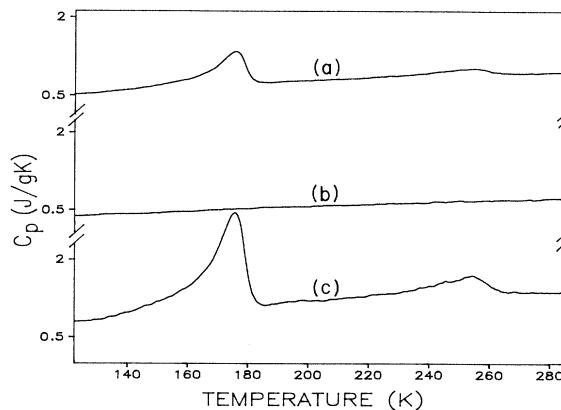


FIG. 1. Differential scanning calorimetry data showing the specific heat ( $C_p$ ) of cyclohexane when restricted in the porous ( $R_p = 4 \text{ nm}$ ) Spherosil sample. The data were collected in the heating mode of the DSC. (a) The specific heat of Spherosil with its pores filled with cyclohexane, (b) the specific heat of Spherosil with its pore filled with helium. The data in Fig. (b) were obtained by vacuum drying the sample of Fig. (a) at 473 K and then filling the pores with helium. (c) The specific heat of physically restricted cyclohexane. The result in Fig. (c) was obtained by subtracting the contributions of the Spherosil sample and the helium.

scanning rate of 15 K/min in the heating mode. For the specific-heat measurements by the DSC technique, well-documented<sup>18–20</sup> procedures were adopted which involved scans of empty volatile pans of equivalent mass, sapphire, and polystyrene (obtained from the National Bureau Standards) as standards, and the sample itself. The weights of the pan, sample, etc., were accurately measured with a microbalance. The accuracy of our calibrated DSC system is  $\pm 1 \text{ K}$  for temperature and 2% for the specific heat. Upon completing the specific-heat measurements on cyclohexane-filled porous Spherosil, the volatile pans were transferred to a vacuum assembly and pumped for 3 h at 473 K to desorb the cyclohexane from the porous silica. After the cyclohexane removal, the specific heat of unfilled porous Spherosil was recorded, enabling us to determine the specific heat of cyclohexane when it is confined in porous material. Figure 1 reproduces the specific heat of the Spherosil ( $R_p = 4 \text{ nm}$ ) sample with its pores filled with cyclohexane, the specific heat of the sample with its pores filled with helium, and the specific heat of cyclohexane when it is physically confined in 4-nm radius pores.

## RESULTS AND DISCUSSION

Figure 2 depicts the observed specific heat ( $C_p$ ) of cyclohexane when it is confined in pores of Spherosil with radii 4, 7.5, 15, 30, and 62.5 nm. For comparison we have also reproduced in Fig. 2 the specific heat of cyclohexane when it is in its bulk form. As can be seen from this figure the  $C_p$  curves of cyclohexane show two

TABLE I. Porous silica properties.

Silica sample	Specific surface area ( $\text{m}^2/\text{g}$ )	Average pore radius (nm)
Spherosil 1	400	4.0
Spherosil 2	200	7.5
Spherosil 3	100	15.0
Spherosil 4	50	30.0
Spherosil 5	25	62.5

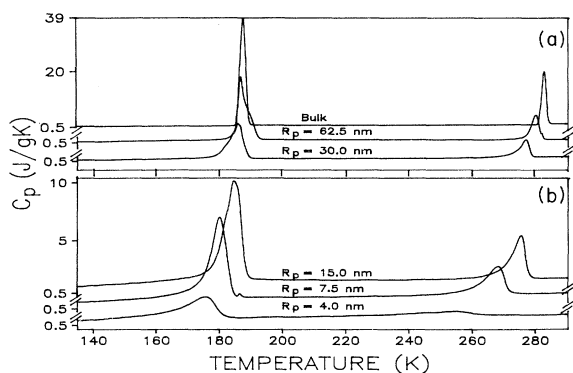


FIG. 2. The specific-heat data showing the effects of pore size on the melting transition (higher temperature peak) and monoclinic-to-cubic structural (lower temperature peak) transition of cyclohexane.

peaks, one at  $T < 187$  K and the other at  $T > 245$  K. Based on the thermodynamic properties<sup>9,10</sup> of bulk cyclohexane we have assumed the former is due to monoclinic-to-cubic structural transition, while the latter is due to the melting transition. The main thermodynamic features of Fig. 2, listed in Table II, can be summarized as follows. (a) Both melting ( $T_{mp}$ ) and solid-solid ( $T_{sp}$ ) transition temperatures<sup>21</sup> are depressed in porous silica relative to the bulk transition (i.e.,  $T_{mo}$  and  $T_{so}$ ) temperatures. The narrower the pores the more depressed are  $T_{mp}$  and  $T_{sp}$ . (b) The extent of the depression of the melting transition,  $\Delta T_{mp}$  ( $\Delta T_{mp} = T_{mo} - T_{mp}$ ), is greater than the extent of the depression in the solid-solid,  $\Delta T_{sp}$  ( $\Delta T_{sp} = T_{so} - T_{sp}$ ), transition. (c) The width (full width at half maximum, FWHM) of the specific heat peaks increases as the pore size decreases. (d) As the pore size decreases, a long tail begins to appear on the low temperature side of the specific heat anomalies due to the melting and the solid-solid transition. This tail becomes much more pronounced for  $R_p < 30$  nm and takes the appearance of a  $\lambda$  shape for a 4-nm-size pore (see Fig. 1). It is worthwhile to point out here that the specific heat curves, showing the melting transition of hydrogen and deuterium in porous ( $R_p = 2.7$  nm) Vycor glass, have similar  $\lambda$ -

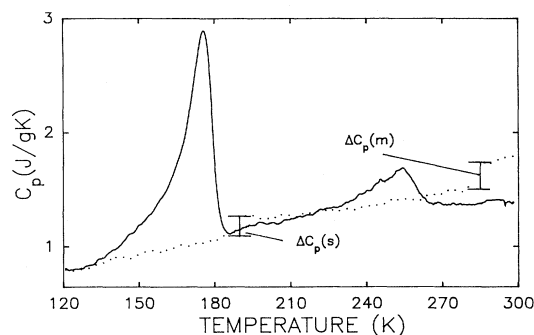


FIG. 3. Comparative specific-heat behavior of bulk (dotted line) and physically confined (in  $R_p = 4$  nm pores, solid line) cyclohexane. The melting and the monoclinic-to-cubic transition regions for bulk cyclohexane have been zapped. The  $\Delta C_p(m)$  and  $\Delta C_p(s)$  are the jumps observed in the specific heat for bulk cyclohexane before and after its melting and solid-solid transition, respectively.

shape anomalies [see Tell and Marris,<sup>2</sup> Figs. 1(a) and 2(a)]. (e) The discontinuity in the specific heat [ $\Delta C_p(m)$ ] is observed for the bulk cyclohexane before and after its melting transition disappears when cyclohexane was confined in pores of size  $R_p \leq 7.5$  nm. This experimental observation is clearly shown in Fig. 3 for a 4-nm-pore Spherosil. Similar to the melting transition, the  $\Delta C_p(s)$  observed for solid-solid transition of bulk cyclohexane also vanishes when cyclohexane was confined in pores of size  $R_p < 30$  nm.

#### Melting transition

Based on geometrical considerations, Warnock *et al.*<sup>1</sup> argue that when a fluid is confined in ultrasmall pores then the supercooling of the fluid will be governed by a single length scale ( $R_p$ ), i.e.,

$$\Delta T_f = \frac{2\Delta\sigma V_m T_0}{\Delta h_f R_p}, \quad (1)$$

TABLE II. The effect of physical confinement on the cyclohexane's thermodynamic properties in porous Spherosils.

Pore size (nm)	Solid-liquid transition				Solid-solid transition			
	$T_{mp}$ (K) <sup>a</sup>	$T_{mp}$ (K) <sup>b</sup>	$\Delta H_m$ (J/g)	FWHM (K) <sup>c</sup>	$T_{sp}$ (K) <sup>a</sup>	$T_{sp}$ (K) <sup>b</sup>	$\Delta H_s$ (J/g)	FWHM (K) <sup>c</sup>
4	241	254	5.6	20	163	176	28.9	12
7.5	261	268	18.1	7	175	180	50.2	6
15	270	271	20.8	6	180	185	59.2	6
30	274	277	25.9	3	183	186	67.5	4
62.5	277	280	28.7	3	185	187	79.9	3
Bulk	281	283	31.9	2	186	188	79.8	2

<sup>a</sup>Onset transition temperature.

<sup>b</sup>Peak transition temperature.

<sup>c</sup>Full width at half maximum.

where  $\Delta h_f$  is the heat of fusion,  $V_m$  the molar volume, and  $\Delta\sigma$  the difference between the solid-wall and liquid-wall interfacial energies. Couchman and Jesser,<sup>22</sup> neglecting the substrate effects, showed that for an ultrasmall isolated one-component collection of noncontiguous metal spheres the surface effects control the melting transition temperature. Arguing that melting transition initiates on the surface of the particles, Couchman and Jesser arrived at an equation for  $\Delta T_m$  which is very similar to Eq. (1), i.e.,

$$\Delta T_m \equiv T_o - T_m = \frac{2\sigma_{sl}VT_o}{\Delta h_f(R-t)}, \quad (2)$$

where subscript sl denotes the solid-liquid interface,  $R$  is the radius of the solid particle (and after melting the radius of the liquid), and  $t$  is the thickness of the liquid around the solid particle. If it is argued that Eq. (2) will also hold for a solid restricted in a porous material then  $\Delta T_{mp}$  of cyclohexane in porous Spherosil should scale with  $(R_p)^{-1}$ . Indeed this is the case as can be seen from Fig. 4. Even though we see a linear relationship between  $\Delta T_{mp}$  versus  $(R_p)^{-1}$ , it is not clear whether the individual parameters involved in Eq. (1) [or Eq. (2)] remain unchanged or the resultant ratio of  $\Delta\sigma V_m / \Delta h_f$  is constant as  $R_p$  varies. The normalized observed enthalpy,  $\Delta H_m$  for the melting transition of 1 g of cyclohexane restricted in porous Spherosil, shows in Fig. 5 that  $\Delta H_m$  changes as the pore radius changes. Also, it appears that the observed  $\Delta H_m$  values are strongly influenced by the total surface area of the porous Spherosils as presented in Fig. 5. There are two possible explanations which can justify the observed reduction in  $\Delta H_m$  as  $R_p$  decreases. One possibility is that the product  $\Delta\sigma V_m$  changes as  $R_p$  changes. The other explanation is that the number of molecules per one gram of cyclohexane, which actually participate in the melting transition, is strongly affected by the pore radius.

As pointed out earlier, cyclohexane is a globular organic compound, and the molecules have considerable rotational motion in the cubic solid ( $186 \text{ K} < T < 280 \text{ K}$ ) phase. Consequently, the intermolecular forces in the cu-

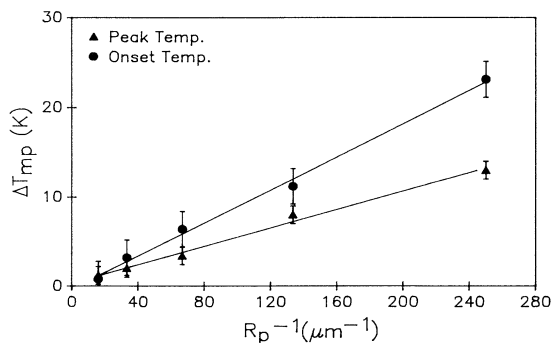


FIG. 4. Graph depicting the linear dependence between the observed melting point depression and  $1/R_p$ .

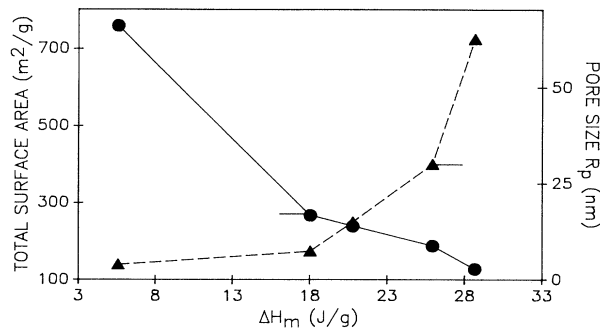


FIG. 5. Graph showing the effects of the pore radius and the total surface area of Spherosil samples on the observed enthalpy of the melting transition of cyclohexane.

bic phase are weak. The Spherosil porous materials being composed of silica are expected to have oxygen atoms on their surface. The hydrogen atoms of cyclohexane can form hydrogen bonds with the oxygen of the Spherosil surface, thus, forming a chemisorbed layer on the porous material surface. However, besides oxygen, the surface of the Spherosil may have other functional groups also present. In an effort to characterize the surface of Spherosil, we recorded the surface sensitive diffuse reflectance-Fourier transform infrared (DR-FTIR) spectra of cleaned and vacuum dried (at 723 K) samples. Our DR-FTIR spectrum of the Spherosil sample showed, besides the expected silica vibrational modes, two additional vibrational bands at 4541 and 3733  $\text{cm}^{-1}$ . The observed vibrations at 4541 and 3733  $\text{cm}^{-1}$  can be assigned to the combination (stretch + bend) and stretching modes of Si-OH groups, respectively.<sup>23</sup> The Si-OH bands were much weaker than the silica bands. The presence of hydroxyl groups, if not uniformly distributed, will further complicate the interaction between the Spherosil surface and the cyclohexane molecules. Based on the observed intensities of silica bands and hydroxyl vibrations, we do not believe the hydroxyl groups are uniformly distributed on the surface. Therefore, the adsorbed structure of cyclohexane is expected to be heterogeneous in the porous Spherosil samples.

In view of the above, it is difficult to see how the variation of the product  $\Delta\sigma V_m$  can be systematic enough to explain the observed trend of  $\Delta H_m$  as a function of  $R_p$ . The surface heterogeneity would induce a distribution in the  $\Delta\sigma$  value. Therefore, only an effective  $\Delta\sigma$  value is operative in Eq. (1) [or Eq. (2)] for cyclohexane confined in porous Spherosil. No systematic trend of the effective  $\Delta\sigma$  value as a function of radius is expected. On the other hand, if there are sites on the surface where cyclohexane is strongly adsorbed and if the adsorbed molecules are not capable of participating in the melting transition, i.e., there are "idle" and "nonidle" cyclohexane molecules, then it is possible to explain the observed  $\Delta H_m$  variation. Under these assumptions that both "idle" and "nonidle" cyclohexane molecules would contribute to the Debye-type part of the specific heat of the cubic phase<sup>8</sup> of

the cyclohexane but only the nonidle molecules would generate the observed enthalpy ( $\Delta H_m$ ), then

$$\Delta H_m = (\Delta h)(N = N_{\text{tot}} - N_{\text{ad}}) . \quad (3)$$

In Eq. (3)  $\Delta h$  is the heat of fusion per freezable molecule,  $N_{\text{tot}}$  the number of molecules in a gram of cyclohexane,  $N$  the number of nonidle molecules, and  $N_{\text{ad}}$  the number of idle molecules. Since the total surface area,  $A$ , of Spherosils for one gram of cyclohexane can be determined by knowing the surface area per gram of silica, Eq. (3) can be further modified by substituting  $N_{\text{ad}} = nA$ .  $n$  is the number of cyclohexane molecules adsorbed on the substrate surface per unit area. Equation (3) can be rewritten as

$$\Delta H_m = N_{\text{tot}} \Delta h - nA \Delta h . \quad (4)$$

Under the strict assumption of idle and nonidle cyclohexane molecules, a linear relationship is expected between  $\Delta H_m$  and the total surface area,  $A$ . An inspection of Fig. 5 shows that there is a linear dependence between the total surface area and  $\Delta H_m$  for 7.5-, 15-, 30-, and 62.5-nm sized pores. Since Eq. (4) is valid for a flat substrate and for a 4-nm sized pore sample, the radius of curvature starts competing with the physical size of the cyclohexane molecule (about 0.61 nm in the cubic phase). Thus, we do not expect  $A$  (for  $R_p = 4$  nm) to fall on the straight line. From the linear relationship of Eq. (4),  $n$  was calculated to be about 19 cyclohexane molecules per  $\text{nm}^2$ . This is equivalent to about 5 layers of adsorbed (idle) cyclohexane molecules in the porous spherosil. The actual number of idle layers is expected to be less than 5 if Awschalom and Warnock's<sup>1</sup> contention is taken into account that the adsorbed layers, especially near the interface of adsorbed and bulklike cyclohexane, may partially participate in the freezing-melting transition. Thus, consistent with the observation of Awschalom and his co-workers,<sup>1</sup> our results also suggest that there are highly viscous layers of fluid near the surface of the porous material. In the case of cyclohexane confined in porous Spherosil, the viscous layers project toward the center of the pore from the surface and are about  $\leq 3$  nm. However, because of the surface heterogeneity, the adsorbed layers would display considerable variation in thickness and orientation. This variation would result in the nucleation of solid grains of various sizes in the porous material, especially for smaller pore sizes, rather than a well-defined, single plug of cubic phase of cyclohexane.

Another interesting feature of the thermodynamic behavior of the melting transition of cyclohexane in porous Spherosil is that the FWHM of the specific heat peak increases as the pore size decreases. This increase in width is accompanied by the appearance of a low-temperature tail in the specific heat peak, due to melting transition. The specific heat peak acquires a  $\lambda$  shape for  $R_p \leq 15$  nm. It may be tempting to assign the observed increased FWHM and the  $\lambda$  shape to the pore-size distribution effect since Eq. (1) predicts larger widths for the larger distribution of  $R_p$ . However, we discount this because (i) the observed FWHM of the solid-solid transition of cyclohexane for the same Spherosil sample is less than the

FWHM of the solid-liquid transition and (ii) the pore distribution predicts a much smaller width than has been observed.<sup>24</sup> An examination of the DSC curves (Fig. 3, Ref. 7), which shows the melting transition of benzene in porous glass, further supports our contention that widths are not only due to the pore-size distribution. The width of the benzene's melting transition is almost four times larger for the 2-nm pore than for the 4.25-nm pore even though the pore-size distributions are 12.8 and 13.5 % for the 2- and 4.25-nm pores, respectively.

The specific heat data of bulk cyclohexane at 120 K  $< T < 300$  K, reproduced in Fig. 3, suggest a jump in  $C_p$  before and after the melting transition, i.e.,  $\Delta C_p(m) (= 0.152 \text{ J/gk})$ . It is well known<sup>11-13,25</sup> that the cyclohexane molecule attains considerable rotational and reorientational motion in the cyclohexane's cubic phase, and the motion is considerably enhanced as the melting transition is approached. Consequently, the heat of fusion is small. As cyclohexane melts, its specific heat in the liquid phase is expected to show a discontinuous jump with respect to the solid phase because of additional degrees of freedom. Our specific heat results on cyclohexane restricted in pores of size 4 and 7.5 nm indicate  $\Delta C_p(m)$  vanishes within our experimental uncertainties. We do observe  $\Delta C_p(m)$  for  $R_p > 7.5$  nm with the magnitude of  $\Delta C_p(m)$  becoming larger with increasing pore size. However, the observed  $\Delta C_p(m)$  for a 62.5-nm-sized pore was still less than the bulk cyclohexane value. Unlike the freezing of fluids in ultrasmall pores, where it has been argued that nucleation does not initiate at the pore walls,<sup>1</sup> the melting of solids is expected to initiate at their surface.<sup>22</sup> If as contended by us, the solid phase of cyclohexane in porous Spherosils has a number of solid grains of various sizes due to the surface heterogeneity of the confining medium, then Eq. (2) predicts the smaller grains of the solid will melt first. We believe the melting will start at the grain boundaries and at the surface of the smaller grains. Since for smaller sized pores ( $R_p < 15$  nm) the radius of curvature would induce additional heterogeneity in the orientation and structure of adsorbed layers, one would expect to have a wider distribution of grain sizes for smaller pores. Hence, one would expect a low-temperature tail in the melting transition of cyclohexane for smaller sized pores. The upper location of the main melting peak would be governed by the size of radius of the confining porous medium since the largest solid grain produced in pores would be less than the diameter of the confining medium. Therefore, the observed larger FWHM and  $\lambda$  shape for smaller sized pores are consistent with our argument that surface effects would result in the growth of various sizes of grains of solids in porous Spherosils. The disappearance of  $\Delta C_p(m)$  of cyclohexane when it is confined in the Spherosils of pores 4 and 7.5 nm is surprising. It may be argued that the number of nonidle cyclohexane molecules in the pores of 4-nm Spherosil is not large enough to detect the  $\Delta C_p(m)$ , due to the resolution of our DSC system. This is certainly possible since a viscous layer (less than 5 monolayers of cyclohexane) is present on the surface. However, it is difficult to see why this should be valid for the 7.5-nm pore Spherosil since the expected  $\Delta C_p(m)$  is about 10%

of the observed  $C_p$  at  $T > 280$  K. If it is agreed that the lack of the observed  $\Delta C_p(m)$  for  $R_p < 15$  nm is not due to the instrument's resolution limitation, then it appears that the effective structure of the liquid phase in the pores  $R_p < 15$  nm is different from the bulk liquid phase. It seems the cyclohexane lacks translational degrees of freedom in 4- and 7.5-nm Spherosil pores, implying a liquid structure of cyclohexane which is much more viscous for smaller sized pores. This conclusion is in qualitative agreement with the observation of Drake and Klafter<sup>3</sup> that the effective viscosity of fluid increases as the pore radius decreases. However, the confirmation of whether cyclohexane confined in pores of size  $R_p < 15$  nm has a much higher viscosity than the bulk will require sensitive specific heat measurements in the heating and cooling modes with either the adiabatic calorimetry or ac calorimetry techniques.

#### Monoclinic-to-cubic structural transition

Cyclohexane undergoes a well-known order-disorder structural transition at 186.1 K.<sup>11,26</sup> At  $T < 186.1$  K, the structure of the solid phase is monoclinic, space group  $C2/c$ , with four molecules per unit cell. At 186.1 K  $< T < 280$  K, the structure is face-centered cubic, space group  $Fm3m$ , with four molecules per unit cell. The magnetic resonance<sup>25</sup> measurements on bulk cyclohexane indicate that at  $T < 155$  K the molecular lattice is effectively rigid with no rotational motion of "chair-shaped" cyclohexane molecules in the lattice. At 155 K  $< T < 186.1$  K, the rotational motion of the cyclohexane molecule about its triad axis sets in. After the solid-solid transition, i.e., at 186 K  $< T < 280$  K, the cyclohexane molecules acquire a rapid reorientational motion and the ability to diffuse in the lattice in the cubic phase. The rapid rotational and reorientational motions of the cyclohexane molecules in the cubic phase renders their effective symmetry to be spherical.<sup>11</sup> Due to the effective extra degrees of freedom in the cubic phase, a jump in the specific heat, i.e.,  $\Delta C_p(s)$ , is expected between the two solid phases (see Fig. 3). Our specific heat measurements on bulk cyclohexane show  $\Delta C_p(s)$  to be 0.1 J/gK. Similar to the  $\Delta C_p(m)$  behavior,  $\Delta C_p(s)$  also vanishes for the solid-solid transition when cyclohexane was confined in Spherosils of pore size 4 nm. It has been argued that if order-disorder transition results in a disordered phase in which the molecules do not have the ability to diffuse but do show substantial reorientational motion then the transition is gradual and the specific-heat curve in the disordered phase is almost a continuation of the ordered phase.<sup>14</sup> Whether cyclohexane molecules lose the ability to diffuse in the cubic phase when restricted in ultrasmall pores cannot be answered from specific heat measurements alone. However, it is reasonable to expect that the surfaces of porous media, especially where the surface-to-volume ratio of the solid is large, would alter the diffusion characteristic of cyclohexane.

As discussed above, the monoclinic-to-cubic transition in cyclohexane is accompanied by reorientational, diffusional, and enhanced rotational motion of cyclohexane molecules in a cubic lattice. This implies bond break-

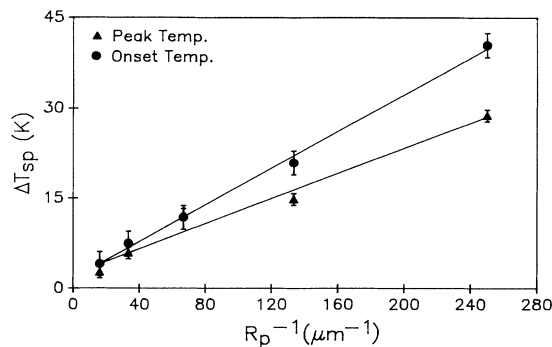


FIG. 6. This graph reproduces the observed depression of the monoclinic-to-cubic transition temperature as a function of  $1/R_p$ .

age and reformation. Consequently, if the surface-to-volume ratio of solid cyclohexane grains become large, then the effective thermodynamics of the solid-solid transition are expected to change. Awschalom and Warnock<sup>1</sup> suggested that Eq. (1) should also hold for a solid-solid transition if the length scale of the solid is an important parameter, i.e.,

$$\Delta T_{sp} \equiv T_{so} - T_{sp} \propto \frac{1}{R_p} \quad (5)$$

Consistent with Eq. (5), the observed  $\Delta T_{sp}$  for monoclinic-to-cubic transition of cyclohexane in porous Spherosils inversely scales with  $R_p$  as graphed in Fig. 6. A similar dependence of  $\Delta T_{sp}$  for  $\gamma - \beta$  solid-solid transition of molecular oxygen has been reported when the oxygen was confined in porous sol-gel glasses.<sup>1</sup> Just like the melting transition, the behavior of  $\Delta H_s$  and FWHM for the solid-solid transition of cyclohexane, as shown in Fig. 7 and listed in Table II, is strongly affected by the total surface area and the pore radius. Attempts were also made, using Eqs. (3) and (4), to determine the nonidle cyclohexane molecules for solid-solid transition in porous Spherosils. Interestingly, the fitting of the observed  $\Delta H_s$  again indicates that about 5 layers of cyclohexane do not

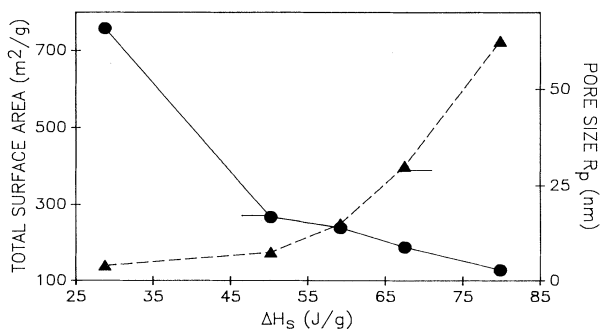


FIG. 7. Graph showing the effects of the pore radius and the total surface area of Spherosil samples on the observed enthalpy of monoclinic-to-cubic transition of cyclohexane.

participate in the monoclinic-to-cubic transition. However, as pointed out for the melting transition, in reality the idle layers are expected to be less than 5.

As argued in the melting transition section, it appears the surface heterogeneity of the confining medium forces cyclohexane to crystallize into a number of small grains in the porous Spherosils rather than into a single crystalline plug. The crystalline grains are expected to have considerable size distribution. For cyclohexane molecules, which have a "chair-shape" and a fairly large size (about 0.61 nm), the radius of curvature of the confining media would induce further disorder in the adsorbed layers. A simple calculation, assuming cylindrical pores and neglecting the surface heterogeneity, shows the angle ( $\theta$ ) between two adjacently adsorbed cyclohexane molecules is governed by

$$\theta = 2 \sin^{-1} \frac{d_c}{d_p}, \quad (6)$$

where  $d_c$  is the effective diameter of the cyclohexane molecule and  $d_p$  the diameter of the confining pore. Thus, as  $R_p$  decreases more disorder will be in the orientation of the adsorbed molecules. In fact,  $\theta$  shows almost a linear dependence with the observed  $\Delta H_s$  and  $\Delta H_m$ .

If there is considerable disorder in the orientation of the adsorbed cyclohexane molecules due to surface heterogeneity and due to the radius of curvature of the confining media, then the observed behavior of  $\Delta H_s$  and FWHM is not inconsistent. A simple view of the observed shape of the specific heat anomaly, owing to the solid-solid transition in porous Spherosil, would be that the disorder in the orientation and the grain size distribution effects are superimposed over the order-disorder characteristics of the transition itself. Under this assumption an effective  $\lambda$  shape for the observed specific heat anomaly is expected. For order-disorder transition, a logarithmic divergence<sup>16,20,27,28</sup> is expected near the transition temperature, i.e.,

$$C_p = A + B \ln \left| \frac{T}{T_{sp}} - 1 \right|. \quad (7)$$

Using the procedure outlined in Refs. 16, 20, and 27, we attempted to fit the excess specific heat (= observed specific heat-background specific heat) data near the observed  $T_{sp}$  to Eq. (7). The logarithmic fitting in the critical regions for  $R_p = 4$  nm and  $R_p = 7.5$  nm sized pore sample was very good with regression coefficients of 0.990 and 0.987, respectively. However, for  $R_p > 7.5$  nm pore size samples the regression coefficients of the loga-

arithmic fit rapidly decreased. It is interesting to point out here that a similar attempt to fit the excess specific heat associated with the melting transition to Eq. (7) was not successful for even  $R_p = 4$  nm pore size sample. Thus, though the melting transition of cyclohexane produces an effective  $\lambda$  shape when restricted in  $R_p < 30$  nm sized pore samples, it still remains a first-order transition.

## SUMMARY AND CONCLUSIONS

We have reported our measurements of the specific heat of cyclohexane in a series of porous Spherosil samples with a view to evaluate how the surface and the confining geometry affect the solid-liquid first-order transition and the solid-solid order-disorder transition of cyclohexane. As expected, the solid-liquid (melting) transition temperature was governed by a single length scale, i.e., the pore radius of the confining Spherosil. However, width and the shape of the specific-heat peak of the melting transition are strongly influenced by the surface heterogeneity of the confining medium. Consistent with the observation of other researchers, our results also indicate that there are rigid layers of the cyclohexane on the surface of the confining medium which do not participate in the melting transition. It seems the translational motion of the cyclohexane molecules, which are confined in porous Spherosil samples, decreases as the pore size decreases. Similar to the melting transition behavior, the transition temperature of the monoclinic-to-cubic order-disorder structural transition is strongly affected by the confining geometry. It is also argued, based on the radius of curvature and the expected surface heterogeneity of the confining Spherosil samples, that solid grains of cyclohexane of various sizes are crystallized in the pores. This variation results in an effective  $\lambda$  shape for the observed melting transition and enhances the low-temperature tail of the order-disorder transition of cyclohexane when cyclohexane is confined in small sized pores.

*Note added in proof.* After this work was submitted, we became aware that Dore *et al.*,<sup>29</sup> from their NMR measurements on cyclohexane confined in 4.5-nm silica pores, have suggested that the enhanced diffusional rates in the porous silica "can be attributed to the highly defective nature of the crystallites forming within the porous medium."

## ACKNOWLEDGMENTS

We would like to thank Professor Aldo Migone for many stimulating discussions and useful suggestions. Authors wish to express their appreciation to Dr. C. L. Jackson for bringing Ref. 29 to their attention.

<sup>1</sup>J. Warnock, D. D. Awschalom, and M. W. Shafer, *Phys. Rev. Lett.* **57**, 1753 (1986); D. D. Awschalom and J. Warnock, *Phys. Rev. B* **35**, 6779 (1987); M. B. Ritter, D. D. Awschalom, and M. W. Shafer, *Phys. Rev. Lett.* **61**, 966 (1988); D. D. Awschalom and J. Warnock, in *Molecular Dynamics in Restricted Geometries*, edited by J. Klafter and J. M. Drake (Wi-

ley, New York, 1989), pp. 351–369.

<sup>2</sup>J. L. Tell and H. J. Maris, *Phys. Rev. B* **28**, 5122 (1983); R. H. Torii, H. J. Maris, and G. M. Seidel, *ibid.* **41**, 7167 (1990).

<sup>3</sup>J. M. Drake and J. Klafter, *Physics Today* **43** (5), 46 (1990).

<sup>4</sup>F. D'Orazio, S. Bhattacharja, and W. P. Halperin, *Phys. Rev. Lett.* **63**, 43 (1989).

- <sup>5</sup>G. K. S. Wang, P. A. Crowell, H. A. Cho, and J. D. Reppy, *Phys. Rev. Lett.* **65**, 2410 (1990).
- <sup>6</sup>R. Mu and V. M. Malhotra, in *Dynamics in Small Confining Systems*, edited by J. M. Drake, J. Klafter, and R. Kopelman, Extended Abstracts EA-22 of Material Research Society, (Material Research Society, Pittsburgh, 1990), pp. 47–50.
- <sup>7</sup>C. L. Jackson and G. B. McKenna, *J. Chem. Phys.* **93**, 9002 (1990); C. L. Jackson and G. B. McKenna, in *Dynamics in Small Confining Systems* (Ref. 6), pp. 31–34.
- <sup>8</sup>M. S. S. Challa, D. P. Landau, and K. Binder, *Phys. Rev. B* **34**, 1841 (1986); R. Marx *ibid.* **40**, 2585 (1989).
- <sup>9</sup>S. C. Mraw and D. F. Naas-O'Rourke, *J. Chem. Thermodyn.* **12**, 691 (1980).
- <sup>10</sup>J. G. Aston, G. J. Szasz, and H. L. Fink, *J. Am. Chem. Soc.* **65**, 1135 (1943).
- <sup>11</sup>R. Kahn, R. Fourme, D. Andre, and M. Rennaud, *Acta Crystallogr. B* **29**, 131 (1973).
- <sup>12</sup>Y. A. Sataty and A. Ron, *Chem. Phys. Lett.* **25**, 384 (1974).
- <sup>13</sup>G. M. Hood and J. N. Sherwood, *Mol. Cryst.* **1**, 97 (1974).
- <sup>14</sup>N. G. Parsonage and L. A. K. Staveley, *Disorder in Crystals* (Clarendon, Oxford, 1978), Chaps. 9 and 10.
- <sup>15</sup>C. L. Guillemin, M. Deleuil, S. Cirendini, and J. Vermont, *Anal. Chem.* **43**, 2015 (1971).
- <sup>16</sup>S. Jasty, P. D. Robinson, and V. M. Malhotra, *Phys. Rev. B* **43**, 13 215 (1991)
- <sup>17</sup>S. Jasty and V. M. Malhotra (unpublished).
- <sup>18</sup>S. C. Mraw, in *Specific Heat of Solids*, edited by C. Y. Ho, CINDAS Data Series on Material Properties (Purdue University, Lafayette, IN, 1988), Vol. I-2, Chap. 11.
- <sup>19</sup>W. W. Wendlandt, *Thermal Analysis* (Wiley, New York, 1986).
- <sup>20</sup>H. J. Frecht, Z. Fu, and W. L. Johnson, *Phys. Rev. Lett.* **64**, 1753 (1990).
- <sup>21</sup>The  $T_{mp}$  and  $T_{sp}$  were determined by picking the maximum point in the respective specific heat anomaly (peak) due to melting and solid-solid transitions. The conventional method (see Ref. 19) of ascertaining the transition temperature by the DSC technique, i.e., the onset temperature, was also done. However, due to the large width and shape of the anomalies in porous silica, the onset temperature is relatively less accurate than the peak temperature.
- <sup>22</sup>P. R. Couchman and W. A. Jesser, *Nature (London)* **269**, 481 (1977).
- <sup>23</sup>A. Jentys, G. Warecka, M. Derewinski, and J. A. Lercher, *J. Phys. Chem.* **93**, 4837 (1989).
- <sup>24</sup>R. Mu and V. M. Malhotra (unpublished).
- <sup>25</sup>E. R. Andrew and R. G. Eades, *Proc. R. Soc. London, Ser. A* **216**, 398 (1953).
- <sup>26</sup>J. Haines and D. F. R. Gilson, *J. Phys. Chem.* **93**, 7920 (1989).
- <sup>27</sup>K. M. Cheung and F. G. Ullman, *Phys. Rev. B* **10**, 4760 (1974).
- <sup>28</sup>E. Pytte and H. Thomas, *Phys. Rev. B* **175**, 610 (1968).
- <sup>29</sup>J. C. Dore, M. Dunn, T. Hasebe, and J. H. Strange, *Coll. Surf.* **36**, 199 (1989).